Universality and scaling in homogeneous compressible turbulence

Diego A. Donzis* and John Panickacheril John
Department of Aerospace Engineering, Texas A&M University, College Station, Texas 77843, USA

(Received 28 September 2019; revised 5 March 2020; accepted 29 July 2020; published 24 August 2020)

Universality in compressible turbulence has proven to be elusive as no unifying set of parameters was found to yield universal scaling laws. This severely limits our understanding of these flows and the successful development of theoretically sound models. Using results in specific asymptotic limits of the governing equations in the absence of a mean flow, we show that universal scaling is indeed observed when the set of governing parameters is expanded to include internally generated dilatational scales regardless of driving mechanisms that produce the turbulence. The analysis, though restricted to homogeneous flows, demonstrates why previous scaling laws fail, and it suggests new venues to identify physical processes of interest and aid in the development of more general turbulence models. We support our results with a new massive database of highly resolved direct numerical simulations along with data from the literature comprising isotropic flows with different forcing mechanisms as well as homogeneous shear flows. We also include flows with considerable bulk viscosity. In search of universal features, we postulate the existence of classes that bundle the evolution of flows in the new parameter space. An ultimate asymptotic regime predicted by renormalization-group theories and statistical mechanics is also assessed with available data.

DOI: 10.1103/PhysRevFluids.5.084609

I. INTRODUCTION

Most flows in nature and engineering are turbulent, exhibiting fluctuations in velocity, pressure, and virtually all hydrodynamic and thermodynamic variables describing the fluid state. In general conditions, which include astrophysical and cosmological contexts, aerodynamics of aircraft and spacecraft, geophysical phenomena such as volcanic eruptions, and combustion systems, among many others, turbulent motions are compressible and one cannot assume a pure solenoidal velocity field as in incompressible turbulence. Due to the extraordinary complexity of these systems with their wide range of nonlinearly interacting spatial and temporal scales, it is only in a statistical sense that these flows are expected to be characterized and understood. Even then, a main obstacle in this endeavor is the apparent difficulty seen in the literature to find universal scaling laws for different flows or for similar flows under diverse conditions. These attempts are commonly based on two nondimensional parameters, namely the Taylor Reynolds number (R_λ), which represents the relative importance of inertial to viscous effects, and the turbulent Mach number (M_t), which is the ratio of a characteristic velocity to the speed of sound. However, these efforts have remained generally inconclusive, and support for different proposals has been limited and often contradictory. In most cases, scaling laws are hard to discern and found to depend on the type of driving mechanism that sustains turbulence [1–7], initial conditions [8,9], or other details of the flow. This is in contrast to the

*donzis@tamu.edu

relative success in incompressible turbulence where universal scaling laws have proven insightful and practically useful [10,11].

As we argue here, universal scaling in compressible turbulence is indeed observed, but only when internally generated scales representing purely compressible motions are the basis for similarity scaling. This represents a departure from previous efforts that focus on externally imposed scales leading to an incomplete set of governing nondimensional parameters to define the state of turbulence. We show how this state of affairs followed from a few (sometimes implicit) assumptions about the variables that control the system.

In particular, we show that to define the state of turbulence, dilatational motions cannot be neglected, as traditionally done. Using first pressure fluctuations, we show that the flow undergoes a transition between two equilibrium states, one dominated by incompressible nonlinear dynamics and the other one by compressible or dilatational motions with simple linear dynamics. The scaling on these two limits depends on different sets of parameters, one including dilatational motions while the other does not. The relative importance of these two equilibria leads naturally to governing parameters that uniquely define the statistical state of fluctuating thermodynamic variables. Classical parameters are also shown to fail to collapse other quantities important to the dynamics of turbulence, such as the rate at which turbulent kinetic energy is dissipated as well as the rate at which vortical motions are produced which exemplify both the nonlinear behavior and conspicuous non-Gaussianity of turbulence. We show that universality is also unraveled for these variables by the introduction of dilatational motions into the governing parameters. These, in turn, define statistical regimes in the extended parameter space, which help explain discrepancies in the literature and explain when and in what sense universal scaling is expected. The results presented thus provide a new perspective for compressible turbulence, and perhaps more general nonlinear multi-scale systems.

II. BACKGROUND

A common paradigm to understand fundamental issues in turbulence is to focus on the intrinsic dynamics of statistically steady isotropic, homogeneous flows to avoid complications from wall effects, spatial nonuniformities, and transients. Even in this simplified setup, the extraordinary difficulties associated with rigorous treatments of the nonlinear governing equations (that is, the Navier-Stokes equations) have resulted in experiments and numerical simulations being a main driver of progress. In the case of compressible turbulence, experiments under these simplifying assumptions in well-controlled conditions are also exceedingly difficult and thus scarce. Therefore, numerical simulations have become a main tool in investigating these flows, in particular direct numerical simulations (DNS) [12,13]. Due to the complexity of the governing equations and the wide range of scales, DNS are computationally extremely expensive and require massive computational power. To the authors' knowledge, the present DNS database is the largest and best-resolved of isotropic compressible turbulence in the published literature.

Because of the comparatively larger body of literature in incompressible turbulence and its more limited set of governing parameters and physical processes, a common approach to study compressible flows is to unveil differences from incompressible counterparts by quantifying departures from known scaling laws [14,15]. A practical, yet rigorous, approach to separate aspects associated with incompressible and compressible motions is the Helmholtz decomposition in which the velocity field is split as $\boldsymbol{u} = \boldsymbol{u}_s + \boldsymbol{u}_d$, where $\boldsymbol{u}_s = \boldsymbol{\nabla} \times \boldsymbol{A}$ ($\boldsymbol{A}$ is the vector potential) and $\boldsymbol{u}_d = \boldsymbol{\nabla}\phi$ (ϕ is the scalar potential). It is trivial to show that $\boldsymbol{u}_s$ is solenoidal (i.e., $\boldsymbol{\nabla} \cdot \boldsymbol{u}_s = \boldsymbol{0}$) and that $\boldsymbol{u}_d$ is irrotational (i.e., $\boldsymbol{\nabla} \times \boldsymbol{u}_d = \boldsymbol{0}$). Since $\boldsymbol{u}_d$ is identically zero in incompressible flows, its existence is ascribed to purely compressibility effects. It is important to note, though, that compressibility can also affect $\boldsymbol{u}_s$. While the decomposition of related variables is also possible (e.g., $\sqrt{\rho}\boldsymbol{u}$ [16]), we have verified that conclusions here are independent of this choice, as discussed later on.

Decades of accumulated numerical work have made some aspects of these flows increasingly clear. A few examples include mixing inhibition due to compressibility [17–19] driven by mean

shear, mixing enhancement for mean irrotational strain [20], changes in decay rates due to the initial level of dilatation or thermodynamic fluctuations [9,21–24], and, when one compares studies as done here, the failure of traditional parameters (in particular Reynolds and turbulent Mach numbers) to provide universal descriptions of these flows.

The purpose of this work is to assess in which sense compressible turbulence can be dubbed universal and under what conditions one can expect universal scaling. In doing so, we propose a set of parameters that define new regimes and lead to universal scaling laws that can indeed collapse all the data available in the literature. This leads to both the recognition of limitations of current approaches as well as new paths for more general understanding and modeling approaches.

III. GOVERNING PARAMETERS, SCALING, AND SIMILARITY

In incompressible flows, the equations for conservation of mass and momentum, known as the Navier-Stokes equations, are sufficient to describe this phenomenon to great accuracy. One can then use a characteristic velocity ($\mathcal{U}$) and length scale ($\mathcal{L}$) to normalize all variables in these equations. Dimensional analysis would then imply that an appropriately normalized statistics of interest, Q, can be represented as $\overline{Q} = f_i(R)$, where an overbar denotes normalization and f_i is presumably a universal function for incompressible flows. Here $R \equiv \rho \mathcal{U} \mathcal{L}/\mu$ is the Reynolds number, where μ is the (constant) dynamic viscosity, and ρ is the (constant) density. Geometrically similar flows at the same R are then expected to have identical properties. In principle, if scaling laws in R are known, then one obtains useful predictive capabilities by simply knowing the geometry and conditions of the flow. Since $\mathcal{L}$ and $\mathcal{U}$ are externally imposed, we can call this *external* similarity.

This approach, however, proves to be limiting when comparisons *across different flows* are attempted since, for example, $\mathcal{L}$ will necessarily correspond to a different length for a wake, jet, or grid turbulence. To compare across flow, it is thus common to use the large-scale Reynolds number $R_L = u_{\rm rms} L/\sqrt{3}\nu$, where $u_{\rm rms}^2 = \langle |\boldsymbol{u} - \langle \boldsymbol{u} \rangle|^2 \rangle$ (angular brackets are suitably defined ensemble averages) is the root-mean-square velocity, and L is the integral length scale or the Taylor Reynolds number $R_\lambda = u_{\rm rms}\lambda/\sqrt{3}\nu$, where λ is the Taylor microscale, which is smaller than $\mathcal{L}$. A vast literature on incompressible turbulence has been devoted to elucidating the scaling of different statistical features of turbulence with R_λ, that is,

$$\overline{Q} = f_i(R_\lambda). \tag{1}$$

Two critical issues are worth noting here. First, there is the implicit assumption that a single velocity scale and a single length scale are enough to completely characterize the flow, at least in a statistical sense. Second, these flow scales ($u_{\rm rms}$, L, and λ) are computed from the flow itself, and their value can only be estimated to within an order of magnitude from *a priori* known geometrical details of the flow setup. One is thus forced to acknowledge the knowledge gap between *a priori* characteristic velocities and lengths from the original geometry, and the resulting *internal* scales from the flow dynamics. When using internally generated characteristic scales, we call this *internal* or *self*-similarity. While a disadvantage of such an approach is the lack of pure predictive capabilities from *a priori* known characteristics of the flow, its advantage lies in its ability to unravel universal aspects across geometrically different flows.

A well-known example is the phenomenology of Kolmogorov [25], who suggested internally generated scales (the Kolmogorov scales) as a way to find universality. One of the most salient examples of its success is the observed collapse of the normalized energy spectrum at different Reynolds numbers and from a variety of flows [10,26,27]. This has played a critical role in understanding and modeling flows in complex realistic situations and in providing the basis for widely used computational approaches including Reynolds-averaged Navier-Stokes (RANS) simulations and large-eddy simulations (LES) [28].

Most efforts to find universality in compressible turbulence have attempted to use known results from incompressible flows and study departures as compressibility levels increase [14]. The degree of compressibility is commonly measured by the Mach number constructed by a characteristic

velocity $\mathcal{U}$, and the speed of acoustic propagation c, that is, $\mathcal{M} \equiv \mathcal{U}/c$. A well-known example of this paradigm is the reduction of the spreading rate of a mixing layer with $\mathcal{M}$ (defined with some average convective velocity) [29]. There is still debate, however, about what is the correct definition of $\mathcal{M}$ [15]. Given the complexity of turbulence in general, and compressible turbulence in particular, a large body of literature has been devoted instead to homogeneous isotropic flows. This approach avoids the additional complexity of geometrical factors, and it allows for a fundamental understanding of intrinsic characteristics that emerge from the governing equations. In such flows, which are the focus of this work as well, it is common to characterize the degree of compressibility with the turbulent Mach number $M_t \equiv u_{\rm rms}/c$, where c is the mean speed of sound. This clearly corresponds to self-similarity, as described above. An implicit assumption here is that the addition of the propagation speed of acoustic waves provides a complete set of governing parameters of the flow. Perhaps a more appropriate interpretation is apparent from the relation $c^2 \sim \langle T \rangle \sim \langle p \rangle / \langle \rho \rangle$ for a perfect gas. Thus, c completes the specification of the thermodynamic state of the flow (at least in a mean sense) when density is included in the set of governing parameters. Note also that using the *mean* speed of sound amounts to again seeking internal similarity as c, in general, depends on the flow solution, which involves temperature fluctuations. Self-similar scaling would then imply that there are universal functions f_c for different nondimensional quantities $\overline{Q}$ in the form [30]

$$\overline{Q} = f_c(R_\lambda, M_t). \tag{2}$$

This has been a basic assumption in a substantial amount of research of compressible flows. For example, several theories have been proposed to determine the scaling of so-called dilatational dissipation [15] or the spectrum [4,7,31] with R_λ and M_t. Weaker formulations of the form $\overline{Q} = f_i(R_\lambda) f_c(M_t)$ are also common. All these different proposals have been tested against numerical simulations with mixed success, and no universal behavior has emerged. Part of this state of affairs, we argue, is because of an incorrect identification of relevant nondimensional groups to determine the statistical state of turbulence. While M_t compares turbulence velocities to the propagation speed of linear waves, it does not contain any information on, for example, the amount on energy in those compressible modes that may propagate in a wavelike fashion.

IV. THE ROLE OF DILATATIONAL MOTIONS

The inadequacy of (2) is evident by the qualitatively distinct behavior observed for turbulence when the nature of the forcing or the initial conditions are changed. The structure and dynamics at both terrestrial and astrophysical conditions were found to depend strongly on whether driving forces [3,16,32] or the initial state of the flow [8,9] contain dilatational contributions.

Consider mass conservation

$$\frac{1}{\rho}\frac{D\rho}{Dt} = -\nabla \cdot \boldsymbol{u}, \tag{3}$$

with D/Dt being the standard substantial derivative. Using Helmholtz decomposition, one can easily see that changes in density following a fluid element can only be due to $\boldsymbol{u}_d$. Thus, it is clear that one needs a dilatational velocity scale, $\mathcal{U}_d$, to properly normalize (3). Furthermore, in many situations, density and pressure are related through an isentropic or polytropic relation [31,33], which would then imply that pressure would also be governed by dilatational motions.

In fact, starting with the full Navier-Stokes equations, one can derive evolution equations for the individual components $\boldsymbol{u}_s$ and $\boldsymbol{u}_d$ [34], where the solenoidal components of velocity and pressure satisfy the incompressible Navier-Stokes equation. The equations for the compressible part of the velocity field are obtained by subtracting the incompressible system from the full set of equations. While these equations are coupled, the time scales and length scales associated with the evolution of each component are expected to be different [24,35]. In fact, for small fluctuations and low Mach numbers, it has been argued that the dilatational component of velocity decouples from its solenoidal component. More formally, and under a slightly different approach, one can linearize the governing

equations, assume isentropic fluctuations, and project the velocity field onto the Craya basis in Fourier space [36]. In this reference frame, the third axis is defined along the wave-number vector $\boldsymbol{k}$, and thus the dilatational velocity projects only along that direction. The solenoidal component is divergence-free, which in Fourier space implies $\hat{\boldsymbol{u}}_s \cdot \boldsymbol{k} = \boldsymbol{0}$ (a caret indicates Fourier transformed variables), and thus it lies on the plane perpendicular to it. Then, to leading order, the dilatational velocity and pressure evolve according to

$$\partial u_d/\partial t = c_0\, k\, P_d, \quad \partial P_d/\partial t = -c_0\, k\, u_d, \tag{4}$$

where u_d can be written as a scalar since the direction is always along the wave-number vector. The speed of sound (constant in this simplified case) and the wave number are c_0 and k, respectively. $P_d = \iota p_d/\rho_0 c_0$ is a normalized pressure with $\iota = \sqrt{-1}$. The problem is now simple enough to accept an analytical solution, which we will explore momentarily. For now, it suffices to say that, at least to first order, the dilatational motions of the governing equations decouple from solenoidal motions, and their dynamics are determined by an interplay between dilatational velocity and pressure. In this approximation, there is no clear reason to believe that a characteristic solenoidal velocity scale would be an appropriate scale for (4). Similar conclusions can be drawn for the evolution of the different modes based on the Kovasznay decomposition [29] or when mean gradients act to couple the two modes [37].

The accumulated data in the literature, in fact, support these arguments, which implies that a relation like Eq. (2) cannot hold in the general case. An example is seen in Fig. 1(a), where we show the variance of pressure normalized by its mean in a statistically steady flow forced stochastically by purely solenoidal forcing (closed circles) and a combination of solenoidal and dilatational forcing (closed triangles). Clearly dilatational forcing has a first-order effect on the dynamics of the flow generating pressure fluctuations that are orders of magnitude larger than those seen at similar M_t with solenoidal forcing. Figure 1 also includes data from a large number of studies, which include solenoidally, dilatationally, and thermally forced isotropic turbulence, as well as shear flows. These are summarized in Table I. It is also clear that the scaling with M_t proposed in [33] for solenoidal forcing (dashed line) is inadequate for the general case when some forcing is in the dilatational mode or when these modes are created due to the thermodynamic coupling between temperature and the dilatational field, as in the case of thermal forcing (diamonds). The latter represent situations such as those involving exothermic chemical reactions in typical turbulent combustion. It has already been noted that M_t cannot collapse the data in a number of situations (see, e.g., [38–40]). This poses a challenge from a modeling perspective, which has led to a need to include additional variables in turbulence models, such as the density variance [40,41], to account for observations. Yet, M_t continued to be used as the intrinsic parameter for compressibility [4,5,7,9,31,33,42–45], mainly due to the lack of any alternate general formalism in the literature. We will see momentarily that universal scaling does in fact emerge when one uses an appropriate nondimensional group that incorporates dilatational motions validated by DNS databases, which cover an extremely wide range of compressibility conditions for forced homogeneous turbulence.

Our data in Fig. 1(a) come from highly resolved DNS of the compressible Navier-Stokes equations representing conservation of mass, momentum, and energy. To provide a full set of closed equations, we use, as is commonly done, a perfect gas to relate thermodynamic quantities, and molecular transport terms with a power-law dependence on temperature. The simulations use tenth-order compact schemes for spatial differentiation, and third-order Runge-Kutta in time. The momentum equations are forced stochastically at the largest scales (low wave numbers) using independent Ornstein-Uhlenbeck random processes with finite-time correlation. In Fourier space, one can project the Fourier modes on a plane perpendicular to the wave-number vector or parallel to it, resulting in solenoidal and dilatational forcing, respectively. A statistically stationary state is maintained by removing energy from the system uniformly through the energy equation. We find the results here to be insensitive to whether energy is removed or not, or the details of energy removal. Further details of the numerical scheme, as well as detailed statistics of the resulting flow, can be found in [31,33].

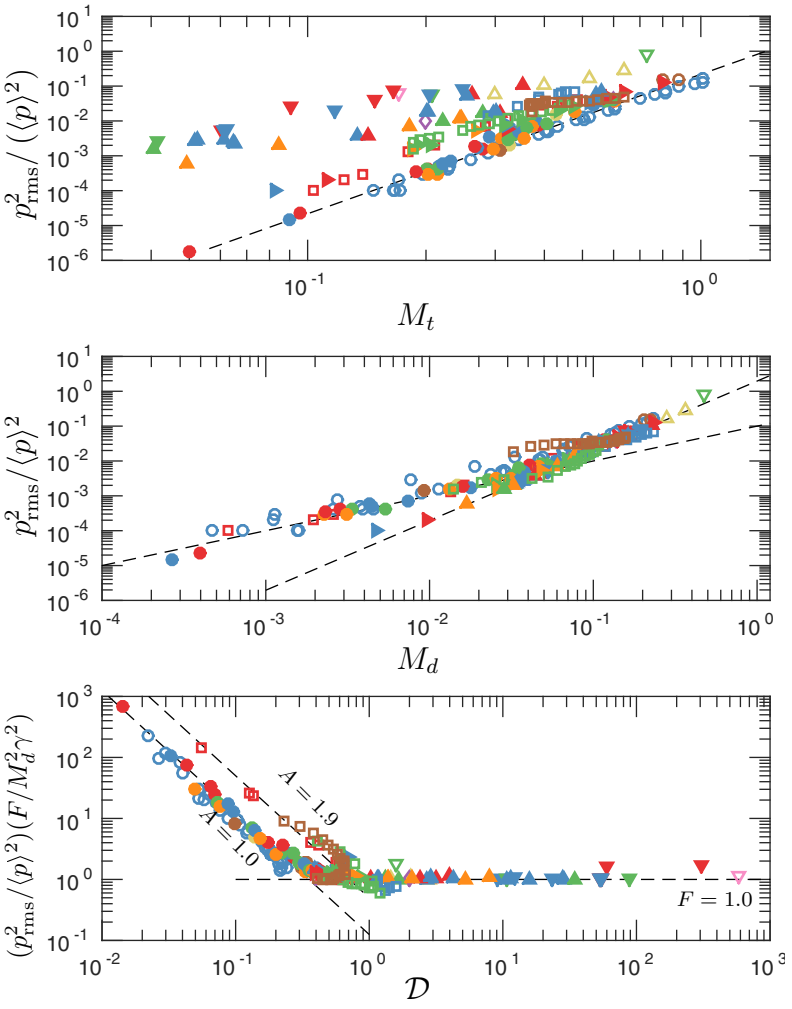

FIG. 1. Scaling of variance of pressure with M_t (a), M_d (b), and $\mathcal{D}$ (c). In (a), dashed lines are $\gamma^2 M_t^4/9$ [33]. In (b), dashed lines are $\gamma^2 M_d^2/F_T$ (high M_d) and $\propto M_d$ for reference (low M_d.) In (c), dashed lines are $\mathcal{D}^{-2}$ (low $\mathcal{D}$) for different values of A and the asymptotic DDE horizontal lines (high $\mathcal{D}$).

V. SELF-SIMILARITY FOR COMPRESSIBLE FLOWS

Returning to the discussion on the general principles around scaling in incompressible turbulence, we are thus confronted with the same difficulties but on a larger parameter space. As argued above, one needs to identify a dilatational velocity $\mathcal{U}_d$ that characterize the content of dilatational motions. Unfortunately, it is unclear how this velocity can be obtained from geometrical aspects of a given flow such as the geometry of a grid. And even if it were possible for one particular flow, the results would typically depend on the details of the setup, as we illustrate below. What we propose instead is to rely on the same approach used in incompressible turbulence, namely to seek internal similarity in which we use an internal scale generated by the flow. A natural choice would be $u_{d,\rm rms}$, the root-mean-square of the dilatational component of velocity based on the Helmholtz decomposition. This is an analogous reasoning that leads to the selection of $u_{\rm rms}$ for incompressible

TABLE I. Databases used in this study. Flow types: homogeneous isotropic turbulence (HIT), which can have solenoidal forcing (S, circles), some dilatational forcing (D, triangles), homogeneous shear turbulence (HST, squares), or thermal forcing (TF). We also include flows (HIT, HST) with different types of gases, in particular two studies with gases for which the ratio of bulk to shear viscosity is 30 (BV) compared to zero for all the other cases. Studies with multiple symbols correspond to the different conditions marked with a † in increasing order. Studies marked with an asterisk did not provide δ and were thus computed using pressure fluctuations and (10).

Flow type	σ	M_t	R_λ	Symbol
HIT, S [7]	100	0.05–1.02	38–370	
HIT, S [16,46]	100	0.11–0.88	12–44	
HIT, S [47,48]	100	1.03	254	
HIT, S (Present)	100	0.05–0.6	38–430 †	
HIT, D [16,46]	0	0.11,0.17	5.4,10	
HIT, D [6]	33.33	0.73	210	
HIT, D [4]	50	0.30–0.65	196–234	
HIT, D [19]	4.76, 50 †	0.6	180	
HIT, D (Present)	70–90	0.04–0.8	30–160 †	
HIT, D (Present)	35–70	0.05–0.55	38–154 †	
HIT, D (Present)	0–35	0.04–0.25	16–77 †	
HST [45]		0.03–0.66	32–220	
HST [49]*		0.2–0.5	16–35	
HST [50]		0.2–0.7 †	14–45	
HST [17]*		0.13–0.65	14–32	
HIT, S, TF [5]	100	0.2,0.6	250	
HIT, S, BV [51]	100	0.1–0.6	100	
HST, BV [51]		0.1–0.6	100	

flows. The parameter space is now augmented such that

$$Q = f(L, \mu, \langle\rho\rangle, u_{\rm rms}, c, u_{d,\rm rms}). \tag{5}$$

Note that only a single length scale is included here, which can be justified on the grounds that the geometry of the device, for example, will provide a natural length scale for the problem with no distinction between solenoidal and dilatational components. Note that this does not necessarily imply that the length scales for the solenoidal and dilatational modes are the same, but instead that the flow will generate its own length scales determined by the parameters in (5). This is an assumption that, while plausible, will ultimately rest on its success in providing universal scaling laws that can collapse numerical and experimental data. This is indeed the case, as we demonstrate in this work.

Dimensional analysis would then reduce the list of parameters in (5) from six to three. Different nondimensional groups can be formed containing dilatational motions. Three such parameters are $\delta = u_{d,\rm rms}/u_{s,\rm rms}$, $\chi \equiv K_d/K$ (where $K_d = \langle\rho|\boldsymbol{u}_d|^2\rangle/2$ and $K = \langle\rho|\boldsymbol{u}|^2\rangle/2$ are the turbulent kinetic energy in the dilatational mode and both modes combined, respectively), and $M_d \equiv u_{d,\rm rms}/c$, which compares a typical velocity of dilatational motions to that of acoustic propagation. The parameter χ is perhaps the most widely used, while M_d has been explored in astrophysical contexts [1]. It is trivial to find relationships such as $\chi \approx \delta^2/(\delta^2+1)$ or $M_d \approx M_t\sqrt{\chi}$, where the approximations stem from neglecting density correlations, which have been verified to be minor for the objectives of this work. Note that searching for the scaling of these parameters with M_t, which has been the focus of some investigations, implicitly assumes them to be dependent parameters of the problem. For example, $\chi \sim M_t^2$ or M_t^4 have been suggested based on different assumptions on EDQNM

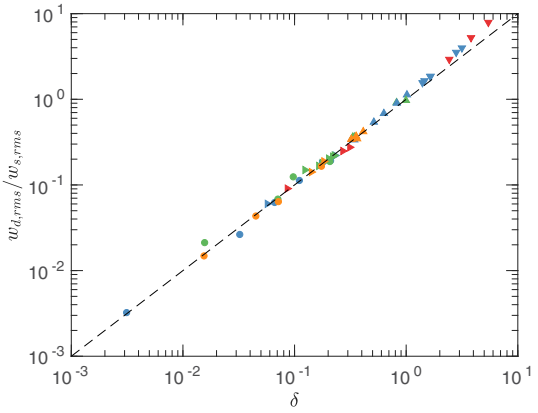

FIG. 2. Scaling of $w_{d,\mathrm{rms}}/w_{s,\mathrm{rms}}$ vs δ where $\boldsymbol{w_d} = \sqrt{\rho}\boldsymbol{u_d}$ and $\boldsymbol{w_s} = \sqrt{\rho}\boldsymbol{u_s}$.

closures [42]. However, as we have seen in Fig. 1(a), M_t and R_λ alone cannot describe completely the statistical state of turbulence in the general case.

Our main objective here is to explore the use of two nondimensional groups such as M_t and δ as the proper similarity parameters. Formally, we suggest that self-similar scaling is possible in compressible flows if internal dilatational scales are included to form similarity parameters. That is, we propose

$$\overline{Q} = f_c(R_\lambda, M_t, \delta) \tag{6}$$

instead of (2) as a base for finding universality in such flows. While other nondimensional parameters can be formed, as discussed above, M_t has been used extensively as a governing parameter, and it is used here complemented by δ.

We note that δ can be alternatively constructed using a density-weighted velocity field w as $\delta = w_{d,\mathrm{rms}}/w_{s,\mathrm{rms}}$, where $\boldsymbol{w} = \sqrt{\rho}\boldsymbol{u}$ [16], $\boldsymbol{w} = \rho^{1/3}\boldsymbol{u}$ [52], or $\boldsymbol{w} = \rho\boldsymbol{u}$ [53]. The differences observed in the value of δ using these different definitions is found to be negligible for all the data considered here, as is evident in Fig. 2. This may not be surprising given that, in view of (3), the effects of density fluctuations may already be incorporated, at least partially, in $\boldsymbol{u}_d$. As an aside, we also note that while these different alternative definitions of δ yield virtually the same results, other statistics may differ. For example, inertial-range characteristics of spectral representations may have distinct behavior depending on whether one looks at the spectrum of $\rho\boldsymbol{u}$, $\sqrt{\rho}\boldsymbol{u}$, or simply $\boldsymbol{u}$ [53], their solenoidal components [54,55], or their dilatational components [56]. Thus, it is important to emphasize that the insensitivity of δ to the different alternatives does not preclude other variables from presenting a different behavior. This is indeed completely analogous to, for example, the use of M_t ($\equiv|\boldsymbol{u}|/\langle c\rangle$) to characterize the flow and assess how spectra using different density-weighted approaches depart from each other as M_t increases.

The addition of δ as a parameter to characterize compressibility highlights another important aspect that may not be immediately apparent. The turbulent Mach number M_t has been traditionally used to characterize two aspects of compressible turbulence. On the one hand, it has been used as a measure of compressibility levels, which can be interpreted as the strength of dilatational motions in the flow. On the other hand, M_t has also been widely interpreted as the ratio of acoustic to turbulent time scales. This follows from using the so-called eddy-turnover time, L/u_{rms}, to characterize the large turbulent scales, and identifying the acoustic time with L/c, which represents the time for an acoustic wave to traverse a distance of the order of the largest scales in the flow. The ratio is obviously M_t and measures the disparity at which acoustic and turbulence processes occur. A large time disparity (low M_t) was assumed to obtain the linear system in (4) [34]. The dual role traditionally assigned to M_t thus conceptually forbids situations in which acoustic phenomena occur

at short time scales (low M_t) but strong compressibility effects (high δ) are present. The alternative use of M_d, χ, or δ to characterize compressibility levels thus does not restrict (4) to flows with small dilatational content.

This may help to explain the accuracy and robustness of equipartition ($F \approx 1$ as shown below) for flows with relatively large values of M_t [24], which is unexpected given that equipartition is based on (4), assumed to be valid only in the low-M_t limit. However, in [24], as the initial M_t was increased, so was χ. It is thus possible that at high χ, dilatational terms in the governing equations may dominate the dynamics even though scale separation was not that large (relatively high M_t). Therefore, the linear system (4) may be valid for a wider range of conditions than originally thought.

VI. THE SCALING OF PRESSURE IN COMPRESSIBLE TURBULENCE

In Fig. 1(a) we showed the dramatic effect of dilatational forcing on the variance of pressure. We have also argued, with (3) and (4), that fluctuations of thermodynamic variables are more closely related to dilatational motions, and we proposed (6). Here we will look at the specific case of pressure fluctuations for which known statistical equilibrium states can be used to justify more rigorously this proposal.

Consider the pressure variance, which according to (6) can be written as $p_{\rm rms}^2/\langle p\rangle^2 = f_c(R_\lambda, M_t, \delta)$, where the mean pressure is formed with the governing parameters as $\langle p\rangle = c^2\langle\rho\rangle/\gamma$. In the incompressible limit it is well-established that pressure finds a statistical equilibrium with $p_{\rm rms} \approx A\langle\rho\rangle u_{s,\rm rms}^2$ with a very weak Reynolds number dependence [57,58]. Using definitions, this expression can be rewritten as

$$p_{\rm rms}^2/\langle p\rangle^2 \approx A^2\gamma^2 M_t^4/9. \tag{7}$$

This scaling has been verified with solenoidally forced simulations in [7,33], also seen in Fig. 1(a) (circles and dashed line).

Now consider the purely dilatational case governed by the system (4). It is easy to obtain an analytical solution for u_d and p_d. For any initial condition, one can show that for unforced flows, the solution tends to an equilibrium state of equipartition between dilatational kinetic energy and potential energy in the dilatational pressure [24], a well-known result also in acoustics [57]. While in the literature this is simply called equipartition, here we will call it p-equipartition to distinguish it from another form of equipartition discussed below. Explicitly, this statistical state can be expressed as $F_p = 1$ using the so-called equipartition function $F_p \equiv c_0^2\rho_0^2 u_{d,\rm rms}^2/p_{d,\rm rms}^2$. While this result involves only the dilatational pressure, Ref. [31] shows that as compressibility levels increase, the dilatational pressure becomes more dominant. This observation implies that at high compressibility levels (a condition to be defined momentarily), the dilatational pressure would indeed be a proxy to assess the scaling of total pressure. In this case, which we term dilatationally dominated p-equipartition, or DDE, we would then expect

$$p_{\rm rms}^2 = c_0^2\rho_0^2 u_{d,\rm rms}^2/F_p \tag{8}$$

or in nondimensional form

$$p_{\rm rms}^2/\langle p\rangle^2 = \gamma^2 M_d^2/F_p. \tag{9}$$

Clearly this scaling does not conform with (2), but it does agree with the proposed (6) since $M_d \approx M_t\delta/\sqrt{\delta^2+1}$. In Fig. 1(b) we test the scaling with M_d. Comparison between parts (a) and (b) reveals a much better collapse of the data on a universal curve at high M_d. Since the database contains cases in which dilatational motions are directly driven by an external dilatational forcing, and also cases in which dilatational motions appear exclusively due to Navier-Stokes dynamics (solenoidal forcing, thermal forcing, or homogeneous shear flows), the collapse in the figure supports the idea of universal scaling when an internal dilatational velocity scale is used, regardless of the means of generation. Reynolds number effects are found to be negligible, consistent with previous studies [31,33]

These results have clear implications for the scaling of compressible turbulence. P-equipartition, as expressed in (9), is a theoretical result that follows from neglecting several terms, including those representing viscous and nonlinear processes, in the governing equations [24]. The fact that p-equipartition is indeed observed at *some* condition (which is identified below) forces us to conclude that (2) is fundamentally deficient in the general case.

By construction, we have $p = p_s + p_d$, which implies $p^2_{\rm rms} = p^2_{s,\rm rms} + p^2_{d,\rm rms} + 2r\, p_{s,\rm rms} p_{d,\rm rms}$, where r is the correlation coefficient between p_s and p_d. In the two asymptotic cases discussed above, however, one component of pressure will be much larger than the other: either $p_{\rm rms} \approx p_{s,\rm rms}$ or $p_{\rm rms} \approx p_{d,\rm rms}$. This will also be the case if the two components of pressure are only weakly correlated, as was found at low M_t [31]. We thus have

$$\frac{p^2_{\rm rms}}{\langle p\rangle^2} \approx A^2\gamma^2 \frac{M_d^4}{\delta^4} + \frac{\gamma^2}{F} M_d^2, \tag{10}$$

or, for convenience, one can rewrite it in nondimensional form as

$$\frac{p^2_{\rm rms}}{\langle p\rangle^2} \frac{F}{M_d^2\gamma^2} \approx A^2 F \mathcal{D}^{-2} + 1, \tag{11}$$

where the new parameter

$$\mathcal{D} \equiv \delta\sqrt{\delta^2 + 1}/M_t \tag{12}$$

is a measure of the relative dominance of the dilatational to the solenoidal contributions. We can also write, in terms of different parameters, $\mathcal{D} = \delta^2/M_d = \sqrt{\chi}/M_t(1-\chi)$. Note that $\mathcal{D}$ is a complex combination of the originally proposed nondimensional groups in (6) and can thus be considered self-similarity of the second kind [59], in which governing nondimensional groups cannot be obtained by dimensional analysis alone.

This relation presents some interesting consequences. First, it suggests that we can indeed expect universal scaling but only when we use the two parameters δ to M_t. Second, it suggests $\mathcal{D}$ as an appropriate parameter to determine not only levels of pressure fluctuations, but also the statistical regime in which one expects turbulence to be. At high $\mathcal{D}$, dilatational pressure dominates, and p-equipartition is the main mechanism governing the dynamics of pressure fluctuations (DDE). At low $\mathcal{D}$, pressure is dominated by its elliptic nature dictated by the incompressible Navier-Stokes equations. Third, in p-equipartition one has $F = 1$, and since $A \sim O(1)$ for all flows, one would expect a critical value $\mathcal{D} = \mathcal{D}_{\rm cr}$ of order unity that separates the two regimes. The specific value of $\mathcal{D}_{\rm cr}$ as well as the asymptote at low $\mathcal{D}$, however, will retain a (weak) dependence on flow characteristics through the constant A.

These observations are indeed consistent with Fig. 1(c), where we show the data normalized according to (11). There is excellent collapse of the data along these two asymptotic equilibrium states with a relatively sharp transition around $\mathcal{D}_{\rm cr} \approx 0.5$. This transition toward a flow dominated by dilatational pressure relative to solenoidal pressure was also observed in Ref. [31] (also included here), though the use of M_t instead of $\mathcal{D}$ (perhaps justified since forcing was solenoidal and identical in nature for all runs) results in larger scatter.

Figure 1(c) also includes thermally forced flows [5] and homogeneous shear flows [17,45,49,50], where no explicit forcing term is added to the governing equations. Instead, turbulent fluctuations are generated as a result of the production mechanism by the mean shear. The good collapse with other data provides further support for universal self-similar scaling for diverse flows driven by different mechanisms.

We do point out, though, that while the constant A in (7) is order unity, its numerical value is flow-dependent. In fact, for the shear flow studies we find $A \approx 1.9$, which is slightly different from 1.2 in stochastically forced isotropic flows [31]. Different low-$\mathcal{D}$ asymptotes are therefore observed for these cases. On the other hand, if full p-equipartition governs the flow ($F = 1$), then the asymptotic state is universal.

To put forth (11), we have assumed that the solenoidal pressure behaves as in incompressible flows and that the dilatational part behaves according to p-equipartition for *all* conditions. This would imply that, for example, $p_{s,\mathrm{rms}} = A\langle\rho\rangle u^2_{s,\mathrm{rms}}$ regardless of the amount of dilatation in the flow. However, weaker assumptions are actually needed, namely that the solenoidal pressure is not affected by the dilatational component when solenoidal pressure dominates the total pressure. Thus, the success of (11) to collapse the data does not preclude other behavior for $p_{s,\mathrm{rms}}$ when dilatational pressure dominates. The same can be said about dilatational pressure, namely that it is not affected by the solenoidal part only when dilatational pressure dominates and that other scaling behavior is possible under those conditions.

Another interesting observation from (12) is the dependence on M_t. While throughout the literature this is considered to be a measure of the level of compressibility, Eq. (12) seems to suggest that an increase in M_t (at constant δ) leads to a decrease in $\mathcal{D}$, which would represent weaker compressibility effects. This result and its broader implications will be discussed in Sec. VIII.

We finally note that in a number of circumstances, low-order statistics of thermodynamic variables can be related to a good approximation by an isentropic, or more generally, polytropic process [4,7,31,33,45,60]. In this case, one finds $T_{\mathrm{rms}}/\langle T\rangle$ and $\rho_{\mathrm{rms}}/\langle\rho\rangle$ to exhibit the same universal scaling seen in Fig. 1(c) with slightly different prefactors.

The spatial structure of the flows in the different regimes is also qualitatively different. In Fig. 3 we show the instantaneous pressure gradient at an arbitrary plane and instant of time. The flow is seen to exhibit completely different features even when M_t is similar [(a) and (d)], showing again the inadequacy of M_t to capture important aspects of the flow. In (a) and (b) ($\mathcal{D} < \mathcal{D}_{\mathrm{cr}}$), we observe that pressure gradient contours look similar to those seen in incompressible turbulence, consistent with the fact that the pressure field is dominated by the solenoidal pressure with finer scale structures becoming more apparent at high Reynolds numbers. Beyond the transitional $\mathcal{D}_{\mathrm{cr}} \approx 0.5$ [panels (c) and (d)], we observe very thin high-pressure gradient fronts resembling shock waves in contrast to the more isotropic vortical high and low gradient regions observed for cases with $\mathcal{D} < \mathcal{D}_{\mathrm{cr}}$. However, some differences are also apparent between panels (c) and (d). The shocklike structures in (c) appear more curved than those in (d), indicating perhaps a stronger coupling between the vortical solenoidal motions and the strong compressions present in the flow. As we argue in the Sec. VIII, this is due to the higher M_t in the former.

VII. SMALL-SCALE UNIVERSAL SCALING

In the classical phenomenology of turbulence, energy is produced at the largest scales (due to the geometry of the device or forcing mechanism). Nonlinear mechanisms then lead to instabilities, which results in the generation of smaller and smaller scales. This energy transfer process continues until scales are small enough that the smoothing effect of molecular transport processes (viscous effects) becomes dominant and the energy is dissipated into heat. In this step-by-step energy cascade, motions progressively lose information from (nonuniversal) geometrical aspects at the large scales. Thus, the hope is for self-similar universality at small scales.

The result of this energy dissipation at small scales is a temperature increase and a decay of all spatial and temporal fluctuations. The rate at which this happens is dictated by the so-called energy dissipation rate $\langle\epsilon\rangle = 2\mu\langle s_{ij}s_{ij}\rangle$ (summation convention implied) where $s_{ij} \equiv (\partial u_i/\partial x_j + \partial u_j/\partial x_i)/2$ is the fluctuating strain rate tensor. Dissipation is also a key ingredient in the classical understanding of turbulent flows as it is the last step in the energy cascade from large scales to small scales [10]. In incompressible homogeneous flows, the dissipation can also be written as $\langle\epsilon\rangle = \mu\langle\omega_i\omega_i\rangle$ (where $\boldsymbol{\omega} \equiv \boldsymbol{\nabla}\times\boldsymbol{u}$ is the vorticity vector) and its scaling has been the focus of a large body of literature [61] and is relatively well understood. A main result is that $\langle\epsilon\rangle$ becomes independent of viscosity at high Reynolds numbers for the flow configurations considered here. In compressible flows, the situation is more complicated and much less is known [31,62] due to both the larger parameter space and the additional terms that contribute to dissipation. In particular, if the flow is homogeneous we can write $\langle\epsilon\rangle = \langle\epsilon_s\rangle + \langle\epsilon_d\rangle$, where $\langle\epsilon_s\rangle \equiv \langle\mu\omega_i\omega_i\rangle$ and $\langle\epsilon_d\rangle \equiv (4/3)\langle\mu\theta^2\rangle$,

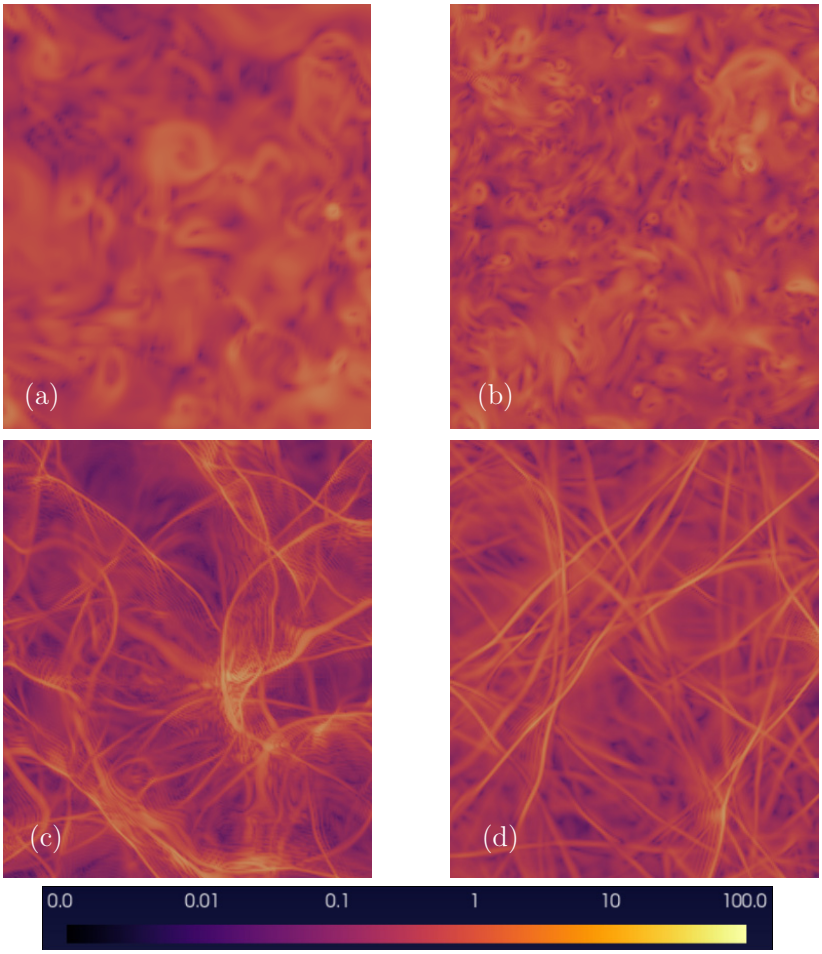

FIG. 3. Contours of $|\nabla p|/|\nabla p|_{\text{rms}}$ for $(\mathcal{D}, R_\lambda, M_t, \delta) = (0.04, 58, 0.09, 0.0035)$ (a), (0.27,102,0.36,0.097) (b), (12,50,0.20,1.4) (c), and (52,51,0.06,1.65) (d).

with $\theta \equiv \partial u_i/\partial x_i$ being the dilatation. The first component is the so-called solenoidal dissipation as its expression is identical to that in incompressible flows. Clearly, only the solenoidal component of the velocity contributes to $\langle\epsilon_s\rangle$ as the dilatational component is irrotational by construction. The second component is the so-called dilatational dissipation and is exclusively due to the dilatational velocity. For fluids with nonzero bulk viscosity, there is an additional term $\langle\mu_v\theta^2\rangle$ (μ_v is the bulk viscosity), but for a fixed value of μ_v/μ [51,63] it is simply proportional to $\langle\epsilon_d\rangle$, in which case it does not require separate modeling.

The historical focus has largely been in understanding and modeling the dilatational dissipation as a "correction" due to compressibility [15]. The most widely used models are of the form $\langle\epsilon_d\rangle \propto \langle\epsilon_s\rangle M_t^\alpha R_\lambda^\beta$, where different models lead to different exponents [e.g., $(\alpha, \beta) = (2, 0)$ [24], $(4, -2)$ [35], or (5,0) [7]], though other more general functional forms of the type $\langle\epsilon_d\rangle = \langle\epsilon_s\rangle F(M_t)$ have also been proposed [15,42]. However, when the available data are collected together as in Fig. 4(a), it is apparent that any model following the similarity scaling in (2) will be unable to capture a universal behavior.

Phenomenologically, since dissipation is proportional to velocity gradients, one can estimate the scaling of each component, in view of (5), as $\langle\epsilon_s\rangle \sim \mu(u_{s,\text{rms}}/L)^2 g_1(R_\lambda, M_t, \delta)$ and

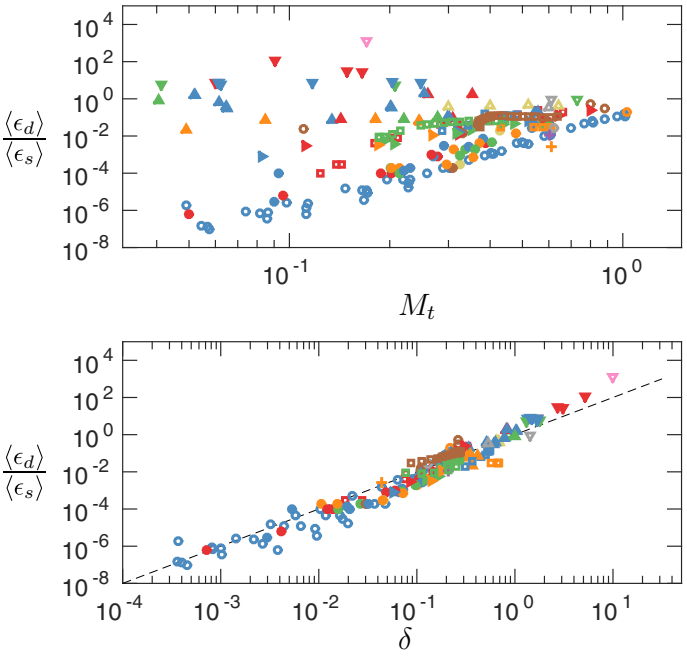

FIG. 4. Scaling of the ratio of dilatational to solenoidal dissipation with (a) M_t and (b) δ. The dashed line in (b) with a slope of 2 is for reference.

$\langle\epsilon_d\rangle \sim \mu(u_{d,\mathrm{rms}}/L)^2 g_2(R_\lambda, M_t, \delta)$, where g_1 and g_2 are some presumably universal scaling functions. The ratio is then $\langle\epsilon_d\rangle/\langle\epsilon_s\rangle = \delta^2 g_3(R_\lambda, M_t, \delta)$, where g_3 is another universal function. In standard models, then, we have $g_3 \propto R_\lambda^\alpha M_t^\beta \delta^{-2}$. To assess the scaling with the governing parameters in Fig. 4(b), we show the ratio of dissipation rates versus δ. We see that all the data from different flows, with different forcing schemes and different conditions, seem to collapse along

$$\langle\epsilon_d\rangle/\langle\epsilon_s\rangle \approx \delta^2 \tag{13}$$

(i.e., $g_3 \approx 1.0$). This scaling seems robust for almost 10 orders of magnitude in $\langle\epsilon_d\rangle/\langle\epsilon_s\rangle$ for all flows (including shear flows and flows with bulk viscosity). While some scatter is observed in the data, no distinguishable systematic trends with the other parameters can be seen. Indeed, some modeling efforts [40,41] included density statistics to account for variations observed in dissipation. The simple scaling proposed in (13) collapses the data better for a wide range of compressibility conditions compared to scaling proposed as a function of density variance and turbulent Mach number [40,41].

This again highlights the inadequacy of (2) and adequacy of (6), and it provides strong support for broad universality when dilatational motions are included in the set of governing parameters. For later use, we note that dilatational dissipation becomes larger than solenoidal dissipation at $\delta \approx 0.9$.

We finally turn to the skewness of longitudinal velocity gradients $S = \langle(\partial u_1/\partial x_1)^3\rangle/\langle(\partial u_1/\partial x_1)^2\rangle^{3/2}$, which has also been studied extensively in incompressible flows [27]. The fact that S is nonzero is a manifestation of the non-Gaussianity of the velocity field. Physically, it represent a normalized measure of the production of rotational motions or enstrophy ($=\langle\omega^2\rangle$) due to nonlinear mechanisms. Its value is found to be an approximately universal constant around -0.5 for a range of incompressible flows at different conditions [27]. In fact, it is so robust a measure that it is common to assess the emergence of "realistic" turbulence by examining the value of S in simulations and experiments. This practice has also been extended to compressible turbulence, though its interpretation is more involved since, at present, it is unknown how S scales with different

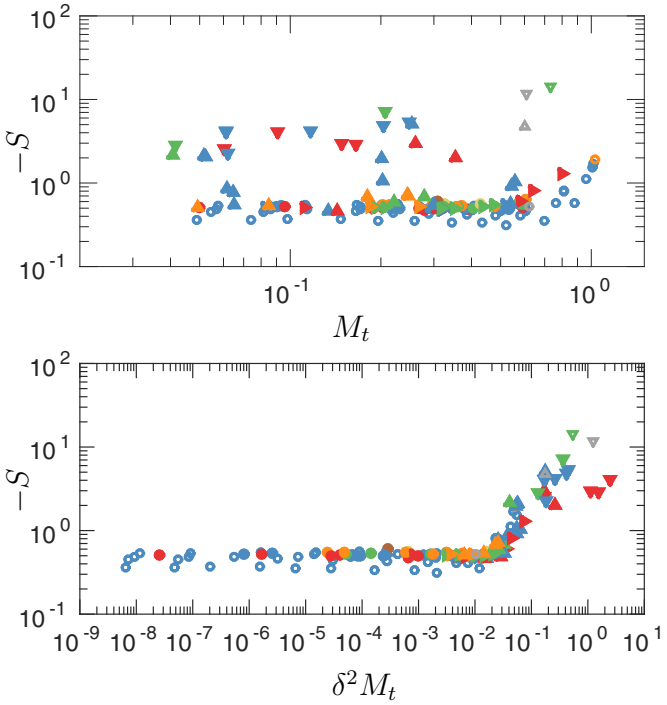

FIG. 5. Skewness of the longitudinal velocity gradient.

parameters. Thus, values not consistent with the incompressible $S \approx -0.5$ could be interpreted as a compressibility effect [7,44,48], as an indication that fully developed turbulence has not been achieved [64], or even as a numerical artifact such as resolution effects [48]. Thus, the search for universal scaling in compressible turbulence also has important practical implications.

In Fig. 5(a), we show the collection of S as a function of M_t. The familiar lack of universality observed before emerges here, too. Under solenoidal forcing and low M_t, S is consistent with its incompressible value, which implies that under these conditions dilatational motions are either very weak or have equal propensity to form both compressions and expansions. A number of authors [7,44,48] have reported larger values of S at higher M_t under solenoidal forcing, which have been attributed to shocklets or small-scale compressions [65]. We see here that under dilatational forcing, large negative skewness is observed even at low M_t, which highlights also the important role of dilatational motions and the need to extend the parameter space.

If the increased dilatational motions are responsible, through shocklets, for the larger value of the gradient skewness, then we would expect wave-steepening mechanisms to be significant. This mechanism is represented by the nonlinear term $\boldsymbol{u}_d \cdot \boldsymbol{\nabla} \boldsymbol{u}_d$. To estimate the order of magnitude of this term, we first note that $\boldsymbol{u}_d$ is of order $u_{d,\mathrm{rms}} \sim \delta u_s$. The multiple scales expansion of [66], in which the solenoidal and dilatational components act at different scales, leads to a split gradient operator $\boldsymbol{\nabla} = \nabla_\eta + M_t \nabla_\xi$, where η and ξ are short- and long-wavelength scales, with the latter corresponding to the acoustic contributions. If we consider only that component, we can estimate the order of magnitude of the nonlinear term as $\delta^2 M_t$. This phenomenological argument would imply that when $\delta^2 M_t$ is high enough, S will increase in magnitude. This is indeed what we see in Fig. 5(b), where, at low values of this parameter, data agree with the incompressible value but diverge at a critical value of $\delta^2 M_t \approx 3 \times 10^{-2}$. This S-divergence at a critical value of $\delta^2 M_t$, though inspired in a somewhat crude order-of-magnitude estimate, is consistent with all other available data in the literature.

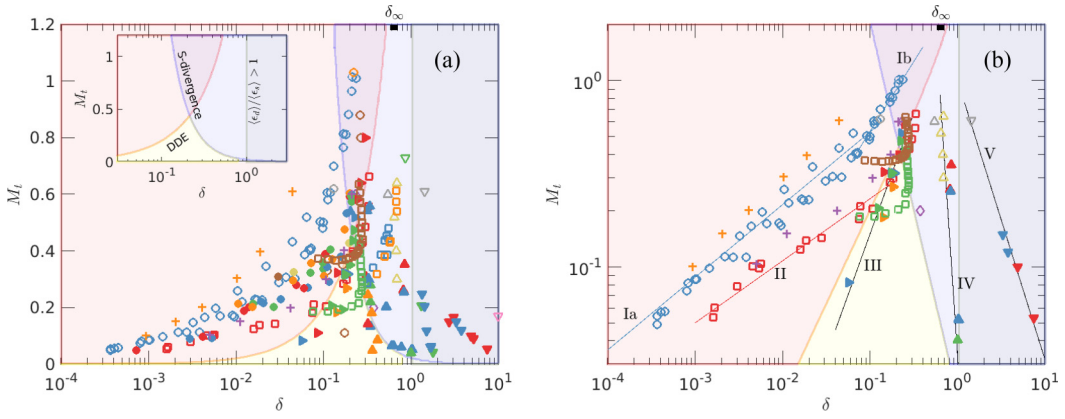

FIG. 6. Regions in the δ-M_t diagram: Dilatationally dominated p-equipartition (DDE, $\mathcal{D} > \mathcal{D}_{\rm cr}$), S-divergence ($\delta^2 M_t > 2 \times 10^{-2}$), and $\langle \epsilon_d \rangle / \langle \epsilon_s \rangle > 1$. (a) Entire database in Table I. (b) Selected trajectories, which include isotropic cases with two types of solenoidal forcing, cases with dilatational forcing, and homogeneous shear flows.

VIII. DISCUSSION: THE BROADER PICTURE

In previous sections, we showed that the statistical state of compressible turbulence cannot be described by the Reynolds and turbulent Mach numbers alone. Instead, a characteristic dilatational velocity needs to be incorporated into the governing parameters to find universal scaling laws. This approach was shown to collapse data for fluctuations of thermodynamic variables, dissipation rates, and skewness of velocity gradients. In doing so, we identified transitions between equilibrium states that can be used to distinguish different regimes. These regimes are shown in the inset of Fig. 6(a) with lines separating dilatationally dominated p-equipartition (DDE), the divergence of skewness, and the dominance of dilatational dissipation. The main part of the figure contains all the data from Table I in the δ-M_t plane.

This figure clearly shows how M_t is unable to determine the state of turbulence in general. Unlike classical problems in critical phenomena, no single transition from "incompressible" to "compressible" can be identified. For example, a flow at low M_t will, as δ increases, first transition to DDE, then it will experience S-divergence, and only at higher levels of δ will dilatational dissipation start dominating the conversion of kinetic energy to internal energy. At higher M_t, on the other hand, S-divergence may occur even before DDE. We see examples of both regimes in Fig. 6(a): the high-M_t ($M_t \gtrsim 0.8$) cases from [7] have much higher values of S than incompressible flows, though pressure is not dominated by dilatational dynamics while our low-M_t ($M_t \lesssim 0.4$) dilatationally forced isotropic cases as well as some intermediate-M_t shear cases [45] are in DDE but S has not diverged yet. Clearly, comparisons between these flows could lead to misleading conclusions, especially if they are at nominally the same M_t.

Note that the S-divergence occurs, except for exceptional conditions (extremely low M_t and high δ), before dissipation is dominated by dilatational motions. If shocklets are responsible for both, as commonly argued, then their contribution to the third-order moment of velocity gradients emerges earlier than that to the second moment. This observation seems to be consistent with recent work [67] suggesting that small-scale high-R_λ features characterized by the anomalous scaling of high-order statistical moments in incompressible flows emerge at lower R_λ than low-order moments. In subsequent work [68], this transition from two statistical steady states (Gaussian at low R_λ and anomalous at high R_λ) provided the key ingredients to obtain the numerical value of the scaling exponents in the anomalous regime. In this context, the discovery of a transition such as that for S (5) is important as it identifies appropriate scaling parameters as well as a seemingly universal

transition point. This could, following [68], provide a fruitful venue to completely characterize small-scale behavior in compressible flows.

The collection of all the data in Fig. 6(a) spans virtually all possible regimes. However, individually, a given flow appears to traverse the δ-M_t space along a specific trajectory. For illustration purposes, we isolate a subset of the database in Fig. 6(b) comprising different flow geometries and type of forcing: the present isotropic simulations with stochastic solenoidal and dilatational forcing, the isotropic flows of [7] with a low-wave-number deterministic forcing, the homogeneous shear flow of [45] and [50], and isotropic simulations with forcing that keeps the ratio of dilatation and solenoidal energy constant at low wave numbers [4].

From Fig. 6(b) we clearly see that different driving mechanisms or geometries and molecular viscous properties generate different levels of dilatations. And for a given flow, this depends on the specific conditions specified by the governing parameters. For example, as the Reynolds and Mach numbers are varied (at constant shear rate) in the HST flows of [45] (red squares), we see an increase in both M_t and δ following an approximate power law of the form $M_t \sim \delta^{1/3}$ (line II) or, equivalently, $\delta \sim M_t^3$ at low δ, but the data appear to transition to the DDE line at $\mathcal{D} = 0.5$ (i.e., $M_t = 0.5\delta\sqrt{\delta^2 + 1}$) as compressibility levels increase, or to a constant δ (more below). This behavior is different from the isotropic data of [7] (blue circles), which follow $\delta \sim M_t^{2.56}$ at low δ (line Ia) and transition to a shallower exponent $\delta \sim M_t^{1.33}$ (line Ib) at higher compressibility levels, never reaching DDE. Compounded with this, the differences in the prefactors in the expressions relating δ and M_t result in order-of-magnitude differences in the value of δ for the same M_t. The trajectory is also different for the isotropic simulation of [4] (yellow triangles), which employs a forcing mechanism that leads to constant δ as M_t is varied. We also include two cases of the temporally evolving shear layers of [50] (green and brown squares) starting from different M_t, respectively. In each case, the flow evolves increasing δ for M_t relatively constant at early times but approaches an approximately vertical line (constant δ) as M_t keeps increasing. Finally, we see that the dilatationally forced cases presented here (right, up, and down triangles for $\sigma = 10\%$, 40%, and 90% dilatational forcing, respectively) present different qualitative behavior. At low dilatational forcing ($\sigma = 10\%$), δ increases as M_t increases (line III), consistent with the other flows, though with a smaller exponent ($\delta \sim M_t^{0.77}$). However, for strongly dilatationally forced flows the trend is the opposite, with δ decreasing with M_t as $\delta \sim M_t^{-0.67}$ (line V). At intermediate dilatational forcing ($\sigma = 40\%$, line IV), δ is approximately constant and close to the data of [4], which were driven by 50% dilatational forcing.

Obviously understanding the detailed physical mechanisms that lead to specific trajectories in the δ-M_t plane is interesting by itself, and their investigation will certainly lead to a deeper understanding of the dynamics of particular flow configurations. Our purpose here, however, is precisely to show that M_t is insufficient to characterize completely the statistical state of turbulence, but that in combination with δ we can obtain, for example, universal scaling laws for the pressure variance, energy dissipation, and skewness of velocity gradients regardless of the generation mechanism.

This general view of universal statistical equilibria for compressible turbulence in the δ-M_t plane can also be used to help contextualize results in the literature. We have pointed out that different flows follow different trajectories. However, it is also possible to distinguish trajectories (or some of its features) that share commonalities for a given *class* of systems. For example, solenoidally forced isotropic turbulence may follow $\delta = CM_t^{\alpha}$ (at least for some region in the δ-M_t plane) with the same exponent α but different prefactors C depending on the specific form of the driving mechanism. This is the case, for example, by comparing flows without and with (plus symbols in the figure) bulk viscosity, which for the same M_t produces weaker dilatational motions [51,63] and thus lower δ. The addition of dilatational forcing changes the numerical value (and even sign) of the scaling exponents α, as discussed above. In support of the concept of classes, we note that data from diverse studies in the literature (see the symbols in Table I) using different forcing and numerical schemes seem to move along the same trajectories (e.g., lines III, IV, and V). Similar considerations could

be applied to shear layers. An implication of this is that, within a class, Eq. (6) reduces to Eq. (2), and proposals in the literature based on M_t may still be approximately valid. The investigation of these trajectories and identification of universal classes would require more data than are currently available from simulations and experiments carefully designed for this purpose. This is obviously an important task that would be extremely valuable in turbulence modeling. The data in Fig. 6, while limited, are in a very broad sense consistent with the existence of classes.

In our search for universal features for compressible turbulence, we finally consider two theoretical results. First, Staroselsky *et al.* [69] studied isotropic compressible turbulence with a Gaussian forcing at large scales using the renormalization group. A statistical equilibrium was found with a constant ratio of solenoidal and dilatational kinetic energy (that is, constant δ) when the forcing spectrum decays sufficiently fast with wave number. In particular, Staroselsky *et al.* predict an asymptotic limit ($\delta \to \delta_\infty$) given by $\delta_\infty^{-2} \approx 3$ or $\delta_\infty \approx 0.58$. This state of equipartition, which is of a different nature from p-equipartition, will be called δ-equipartition. The second, but earlier, study is that of Kraichnan [70], who also suggested δ-equipartition but based on statistical mechanics principles. In particular, based on the Liouville theorem, Kraichnan suggested that in the inviscid case and with weak excitation there is equipartition between vortical solenoidal modes (with two degrees of freedom) and acoustic modes, also with two degrees of freedom (one from the dilatational mode and one from a bijective function of the density mode). Thus, $\delta_\infty^2 = 1/2$ or $\delta_\infty = 0.7$, which is not far from [69], though derived from a completely different perspective. It is interesting that in the case of weak fluctuations of thermodynamic variables, the more general formulation of Kraichnan also leads to a form of p-equipartition.

The range formed by these two theoretical limits is marked on the top of both panels of Fig. 6 with a thick line. Collectively, the data seem qualitatively consistent with such a limit as a universal feature across flows. For example, we see this trend in naturally forced flows such as the shear layers of [50] where δ clearly approaches a constant not far from the theoretical prediction (apparently independent of initial M_t) as M_t increases during the temporal evolution of the flow. This same behavior with apparently the same asymptotic δ is also observed for shear layers with bulk viscosity 30 times larger than the shear viscosity [51], even though, as pointed out in that work, they exhibit weaker dilatational motions than flows with zero bulk viscosity at the same Mach number. Solenoidally forced isotropic flows (with or without bulk viscosity) also exhibit a trend toward the same constant, though for this class of flows the asymptote seems to be attained at higher M_t. It is also interesting that in our isotropic simulations, when dilatational forcing is strong and kept constant, and temperature and viscosity are varied to achieve higher M_t, δ decreases [line IV in Fig. 6(b)]. Even with purely dilatational forcing, the values of δ seem bounded as M_t increases. Further support for such a universal asymptotic behavior is provided by the very-high-M_t simulations of [1] that, while different from all in Table I since they are based on the Euler equations and the flow is isothermal, yield $\delta \approx 0.5$, very close to the theoretical predictions, as M_t is increased to values as high as 15. Thus, it is possible that this represents a more general universal ultimate regime at high M_t. It would be interesting to investigate these questions with other theoretical approaches such as EDQNM or DIA [42]. In particular, simulations based on EDQNM-DIA are known to depend on the specific choice of the decorrelation damping factor at low M_t. The ideas and results we put forward in this work can be helpful in guiding this selection process.

The observations above can shed light on the proper interpretation of the governing parameters. In the traditional interpretation, M_t is a measure of both separation of time scales and compressibility level. As we argued above, this is inadequate. Instead, δ is the appropriate nondimensional group that represents compressibility levels (dilatational motions), while M_t represents the ratio of time scales. When a vast disparity of time scales is present, one would expect little interaction between solenoidal and dilatational phenomena. In fact, when the equations of motion are decomposed into solenoidal and dilatational modes, the expansion of [66] suggests that the cross-terms responsible for the energy exchange between the two modes grow with M_t. Thus, a simple physical picture emerges based on a universal δ-equipartition state: if flow conditions are such that $\delta \neq \delta_\infty$, then an increase of M_t will lead to stronger nonlinear interactions between solenoidal and dilatational

modes that would enable stronger redistribution of energy toward a complete δ-equipartition [70]. If $\delta < \delta_\infty$, the stronger interaction will lead to transfers from the solenoidal to the dilatational mode. If $\delta > \delta_\infty$, the transfer would proceed in the opposite direction. This phenomenological argument is consistent with the data in Fig. 6 and also with the observations made about the stronger interaction of vortical motions with compression waves giving rise to the more curved spatial structures in Fig. 3 at higher M_t but the same δ. Rigorous studies of energy transfers from the governing equations are certainly warranted. It is also interesting, and perhaps counterintuitive, to see that at high M_t ($M_t > \delta_\infty\sqrt{\delta_\infty^2 + 1}/\mathcal{D}_{\rm cr} \approx 1.34$), δ_∞ is to the left of the DDE line. Thus, if δ-equipartition is indeed a universal asymptote at high M_t, then the solenoidal component will always dominate pressure, regardless of how high M_t is. In fact, the higher M_t is, the more dominant solenoidal pressure becomes ($\mathcal{D}$ decreases) as one traverses the δ-M_t plane with $\delta = \delta_\infty$.

We finally note that our results also point to some interesting additional considerations regarding the multiscale nature of interactions in compressible turbulence. For example, we showed that the new parameter $\mathcal{D}$ governs p-equipartition but in a weak sense [42], that is, on the variance of pressure fluctuations whose main contributions come from large scales. However, it is possible and indeed observed that while large scales can be in p-equipartition, small scales can be in other kinds of equilibria [7]. Another example is the scaling of the ratio of dissipation components with δ. Here, a parameter describing the relative content of dilatational motions at large scales (δ) provides an accurate description of the relative importance of processes at small scales (i.e., dissipation). While not surprising for the solenoidal component due to the so-called dissipative anomaly [31], the good collapse of the data may indicate a scale-to-scale cascade process for dilatational motions as well. This, in turn, has implications on the spectral distributions, which are expected to have different spectral behavior in different regions of the δ-M_t plane. This is evident as one examines, for example, the qualitative change in the spatial structure of flow fields in Fig. 3 as one moves from (a) to (d), where ultimately the dilatational component dominates the pressure field. Thus, one can speculate about some of the expectations in different regions of the δ-M_t plane.

Consider first the region with $\mathcal{D} > 0.5$, which, as we have shown, corresponds to p-equipartition: the variance of dilatational pressure is in equipartition with that of the dilatational velocity field ($F_p = 1$). Because of Parseval's theorem and the fact that the spectrum of pressure and velocity decays fast with wave number, this would then imply that the low-wave-number part of the spectrum of the dilatational velocity, $E_d(k)$, coincides with that of dilatational pressure, $E_{pd}(k)$, when normalized in a way similar to (8) for low-wave-number modes. This is indeed observed from our DNS data. In fact, as $\mathcal{D}$ increases, one may expect an increasingly wider range of wave numbers in the spectrum to be in p-equipartition. When the entire spectrum is in p-equipartition, that is, $E_{pd}(k) = \langle c\rangle^2\langle\rho\rangle E_d(k)$ for all k, the flow is said to be in *strong* p-equipartition [42]. This is indeed supported by DNS data as one moves across iso-$\mathcal{D}$ lines. Another example of how the results here can help understand spectral distributions is in cases in which solenoidal pressure dominates (i.e., $\mathcal{D} < 0.5$). It has been suggested that at low M_t, the flow may be described by pseudosound theory [35,42] in which dilatational motions are slaved to solenoidal motions. This results in a number of predictions including $\langle\epsilon_d\rangle/\langle\epsilon_s\rangle \sim M_t^4$ and a k^3 spectrum [7]. However, in all studies only M_t was used to assess the conditions under which pseudosound is applicable and no universal M_t was found to describe the transition to pseudosound. For example, Ref. [7] suggests a transition at $M_t \approx 0.4$ while in [45] it is at $M_t \approx 0.1$ based on the scaling of $\langle\epsilon_d\rangle/\langle\epsilon_s\rangle$. In fact in [51], for flows with bulk viscosity, no transition was observed and pseudosound scaling is valid for M_t as high as 0.6. Note that the scaling of dissipation depends on the scaling of the energy spectrum at high wave numbers. This is clearly seen in [7], where an increasingly wide range of the (high-wave-number) spectrum agrees with pseudosound predictions as M_t is decreased. The results of our work here can now be used to delimit a potential pseudosound region in the δ-M_t plane. For this, we note that pseudosound can happen when the solenoidal pressure dominates $\mathcal{D} < 0.5$ and when the dilatational motions are driven entirely by the solenoidal motions. For this to happen, one can argue that this process should not be modified by a dilatational cascade that can redistribute energy across scales. A measure of the strength of this dilatational cascade is the skewness of velocity gradients, which, as

we have shown, remain at their incompressible value when $\delta^2 M_t < 10^{-2}$. Beyond that point, we see much larger values of S—the so-called S-divergence. Thus, one can speculate that the dissipative range of the spectrum (and thus the average dissipation rate) would agree with pseudosound when $\mathcal{D} < 0.5$ and $\delta^2 M_t < 10^{-2}$. By examining the data in the literature, in particular Refs. [7,45,51], we find that this criterion indeed agrees with the ranges proposed for pseudosound in those studies. In fact, we can also see that as $\delta^2 M_t$ decreases further from the transition, a wider range of wave numbers agree with pseudosound scaling as noted in [7]. While more detailed analysis is necessary to assess the full scaling of the spectrum at different conditions, the two examples discussed briefly here (p-equipartition and pseudosound) provide an illustration of how the δ-M_t plane can help also in characterizing other quantities of interest, such as spectra.

In conclusion, we show that universal scaling laws can indeed be identified for compressible turbulence if dilatational motions are incorporated in the nondimensional groups used to determine its statistical equilibrium state. This is supported by a large database of new direct numerical simulations of isotropic compressible turbulence with different driving mechanisms combined with an extensive set of flows in the literature. Whereas the traditional turbulent Mach number fails to describe the state of the turbulence and thus to collapse the data for different conditions and flows, we proposed a δ-M_t plane in which different statistical equilibria can be identified, regardless of the flow configuration and geometrical details. Different flows traverse this plane in different ways, but one can postulate classes of systems that may share universal trajectories or scaling exponents defining those trajectories. An ultimate asymptotic regime predicted by renormalization group and statistical mechanics is not inconsistent with available data. The successful collapse of all the available data (pressure variance, energy dissipation, enstrophy generation), and the identification of the proper parameters to encounter universal scaling laws, open the door to both accurate models and a deeper understanding of compressible turbulence.

ACKNOWLEDGMENTS

The authors gratefully acknowledge support from the National Science Foundation (Grant No. 1605914) and from the Extreme Science and Engineering Discovery Environment (XSEDE) and the Texas Advanced Computating Center (TACC) for computational resources.

[1] L. Konstandin, P. Girichidis, C. Federrath, and R. S. Klessen, A new density variance—Mach number relation for subsonic and supersonic isothermal turbulence, Astrophys. J. **761**, 149 (2012).
[2] C. Federrath, R. S. Klessen, and W. Schmidt, The density probability distribution in compressible isothermal turbulence: Solenoidal versus compressive forcing, Astrophys. J. Lett. **688**, L79 (2008).
[3] C. Federrath, R. S. Klessen, and W. Schmidt, The fractal density structure in supersonic isothermal turbulence: Solenoidal versus compressive energy injection, Astrophys. J. **692**, 364 (2009).
[4] J. Wang, M. Wan, S. Chen, C. Xie, and S. Chen, Effect of shock waves on the statistics and scaling in compressible isotropic turbulence, Phys. Rev. E **97**, 043108 (2018).
[5] J. Wang, M. Wan, S. Chen, C. Xie, L-P Wang, and S. Chen, Cascades of temperature and entropy fluctuations in compressible turbulence, J. Fluid Mech. **867**, 195 (2019).
[6] J. Wang, Y. Yang, Y. Shi, Z. Xiao, X. T. He, and S. Chen, Statistics and structures of pressure and density in compressible isotropic turbulence, J. Turbul. **14**, 21 (2013).
[7] J. Wang, T. Gotoh, and T. Watanabe, Spectra and statistics in compressible isotropic turbulence, Phys. Rev. Fluids **2**, 013403 (2017).
[8] S. Pirozzoli and F. Grasso, Direct numerical simulations of isotropic compressible turbulence: Influence of compressibility on dynamics and structures, Phys. Fluids **16**, 4386 (2004).
[9] R. Samtaney, D. I. Pullin, and B. Kosovic, Direct numerical simulation of decaying compressible turbulence and shocklet statistics, Phys. Fluids **13**, 1415 (2001).
[10] U. Frisch, *Turbulence* (Cambridge University Press, Cambridge, 1995).

[11] K. R. Sreenivasan, Turbulent mixing: A perspective, Proc. Natl. Acad. Sci. (USA) **116**, 18175 (2018).
[12] P Moin and K Mahesh, Direct numerical simulation: A tool in turbulence research, Annu. Rev. Fluid Mech. **30**, 539 (1998).
[13] T. Ishihara, T. Gotoh, and Y. Kaneda, Study of high-Reynolds number isotropic turbulence by direct numerical simulation, Annu. Rev. Fluid Mech. **41**, 165 (2009).
[14] S. K. Lele, Compressibility effects on turbulence, Annu. Rev. Fluid Mech. **26**, 211 (1994).
[15] T. B. Gatski and J-P. Bonnet, *Compressibility, Turbulence and High Speed Flow*, 2nd ed. (Elsevier, Amsterdam, 2013).
[16] S. Kida and S. A. Orszag, Energy and spectral dynamics in forced compressible turbulence, J. Sci. Comput. **5**, 85 (1990).
[17] S. Sarkar, The stabilizing effect of compressibility in turbulent shear flow, J. Fluid Mech. **282**, 163 (1995).
[18] A. W. Vreman, N. D. Sandham, and K. H. Luo, Compressible mixing layer growth rate and turbulence characteristics, J. Fluid Mech. **320**, 235 (1996).
[19] Q. Ni, Compressible turbulent mixing: Effects of compressibility, Phys. Rev. E **93**, 043116 (2016).
[20] C. Cambon, G. N Coleman, and N. N Mansour, Rapid distortion analysis and direct simulation of compressible homogeneous turbulence at finite mach number, J. Fluid Mech. **257**, 641 (1993).
[21] D. S. Praturi and S. S. Girimaji, Effect of pressure-dilatation on energy spectrum evolution in compressible turbulence, Phys. Fluids **31**, 055114 (2019).
[22] G. A. Blaisdell, N. N. Mansour, and W. C. Reynolds, Compressibility effects on the growth and structure of homogeneous turbulent shear-flow, J. Fluid Mech. **256**, 443 (1993).
[23] J. R. Ristorcelli and G. A. Blaisdell, Consistent initial conditions for the DNS of compressible turbulence, Phys. Fluids **9**, 4 (1997).
[24] S. Sarkar, G. Erlebacher, M. Y. Hussaini, and H. O. Kreiss, The analysis and modeling of dilatational terms in compressible turbulence, J. Fluid Mech. **227**, 473 (1991).
[25] A. N. Kolmogorov, Local structure of turbulence in an incompressible fluid for very large Reynolds numbers, Proc. R. Soc. London A **434**, 9 (1991).
[26] A. S. Monin and A. M. Yaglom, *Statistical Fluid Mechanics, Vol. II* (MIT Press, Cambridge, MA, 1975).
[27] K. R. Sreenivasan and R. A. Antonia, The phenomenology of small-scale turbulence, Annu. Rev. Fluid Mech. **29**, 435 (1997).
[28] P. Sagaut, *Large Eddy Simulation for Incompressible Flows: An Introduction* (Springer Science & Business Media, Berlin, Heidelberg, 2006).
[29] A. J. Smits and J. P. Dussauge, *Turbulent Shear Layers in Supersonic Flow* (Springer, New York, USA, 2006).
[30] A more general list of parameters would include the ratio of specific heats, γ, but it is not included here for simplicity.
[31] S. Jagannathan and D. A. Donzis, Reynolds and Mach number scaling in solenoidally-forced compressible turbulence using high-resolution direct numerical simulations, J. Fluid Mech. **789**, 669 (2016).
[32] W. Schmidt, C. Federrath, M. Hupp, S. Kern, and J. C. Niemeyer, Numerical simulations of compressively driven interstellar turbulence, Astron. Astrophys. **494**, 127 (2009).
[33] D. A. Donzis and S. Jagannathan, Fluctuations of thermodynamic variables in stationary compressible turbulence, J. Fluid Mech. **733**, 221 (2013).
[34] G. Erlebacher, M. Y. Hussaini, H. O. Kreiss, and S. Sarkar, The analysis and simulation of compressible turbulence, Theor. Comput. Fluid Dyn. **2**, 73 (1990).
[35] J. R. Ristorcelli, A pseudo-sound constitutive relationship for the dilatational covariances in compressible turbulence, J. Fluid Mech. **347**, 37 (1997).
[36] A. Simone, G. N. Coleman, and C. Cambon, The effect of compressibility on turbulent shear flow: A rapid-distortion-theory and direct-numerical-simulation study, J. Fluid Mech. **330**, 307 (1997).
[37] D. Livescu and C. K. Madnia, Small scale structure of homogeneous turbulent shear flow, Phys. Fluids **16**, 2864 (2004).
[38] M. Danish, S. S. Sinha, and B. Srinivasan, Influence of compressibility on the lagrangian statistics of vorticity–strain-rate interactions, Phys. Rev. E **94**, 013101 (2016).

[39] S. S. Parashar, N. Sinha, M. Danish, and B. Srinivasan, Lagrangian investigations of vorticity dynamics in compressible turbulence, Phys. Fluids **29**, 105110 (2017).
[40] F. Hamba and G. A. Blaisdell, Towards modeling inhomogeneous compressible turbulence using a two-scale statistical theory, Phys. Fluids **9**, 2749 (1997).
[41] A. Yoshizawa, Three-equation modeling of inhomogeneous compressible turbulence based on a two-scale direct-interaction approximation, Phys. Fluids A **2**, 838 (1990).
[42] P. Sagaut and C. Cambon, *Homogeneous Turbulence Dynamics* (Springer, Cham, Switzerland, 2018).
[43] J. R. Ristorcelli, Passive scalar mixing: Analytic study of time scale ratio, variance, and mix rate, Phys. Fluids **18**, 075101 (2006).
[44] J. Wang, T. Gotoh, and T. Watanabe, Shocklet statistics in compressible isotropic turbulence, Phys. Rev. Fluids **2**, 023401 (2017).
[45] S. Chen, J. Wang, H. Li, M. Wan, and S. Chen, Spectra and Mach number scaling in compressible homogeneous shear turbulence, Phys. Fluids **30**, 065109 (2018).
[46] S. Kida and S. A. Orszag, Energy and spectral dynamics in decaying compressible turbulence, J. Sci. Comput. **7**, 1 (1992).
[47] J. Wang, Y. Shi, L-P Wang, Z. Xiao, X. T. He, and S. Chen, Scaling and Statistics in Three-Dimensional Compressible Turbulence, Phys. Rev. Lett. **108**, 214505 (2012).
[48] J. Wang, Y. Shi, L.-P Wang, Z. Xiao, X. He, and S. Chen, Effect of shocklets on the velocity gradients in highly compressible isotropic turbulence, Phys. Fluids **23**, 125103 (2011).
[49] S. Sarkar, G. Erlebacher, and M. Y. Hussaini, Direct simulation of compressible turbulence in a shear flow, Theor. Comput. Fluid Dyn. **2**, 291 (1991).
[50] S. Sarkar, G. Erlebacher, and M. Y. Hussaini, Compressible homogeneous shear: Simulation and modeling, in *Turbulent Shear Flows*, edited by F. Durst (Springer, Berlin, Heidelberg, 1993), Vol. 8, pp. 249–267.
[51] S. Chen, X. Wang, J. Wang, M. Wan, S. Li, and H. Chen, Effects of bulk viscosity on compressible homogeneous turbulence, Phys. Fluids **31**, 085115 (2019).
[52] A. G. Kritsuk, M. L. Norman, P. Padoan, and R. Wagner, The statistics of supersonic isothermal turbulence, Astrophys. J. **665**, 416 (2007).
[53] H. Aluie, Scale decomposition in compressible turbulence, Physica D **247**, 54 (2013).
[54] J. Panickacheril John, D. A Donzis, and K. R. Sreenivasan, Solenoidal Scaling Laws for Compressible Mixing, Phys. Rev. Lett. **123**, 224501 (2019).
[55] J. P. John, D. A. Donzis, and K. R Sreenivasan, Compressibility effects on the scalar dissipation rate, Combust. Sci. Technol. **192**, 1320 (2020).
[56] D. Zhao and H. Aluie, Inviscid criterion for decomposing scales, Phys. Rev. Fluids **3**, 054603 (2018).
[57] L. D. Landau and E. M. Lifshitz, *Fluid Mechanics* (Pergamon, Kidlington, Oxford, UK, 1987).
[58] D. A. Donzis, K. R. Sreenivasan, and P. K. Yeung, Some results on the Reynolds number scaling of pressure statistics in isotropic turbulence, Physica D **241**, 164 (2012).
[59] G. I. Barenblatt and Y. B. Zeldovich, Self-similar solutions as intermediate asymptotics, Annu. Rev. Fluid Mech. **4**, 285 (1972).
[60] J. Wang, T. Gotoh, and T. Watanabe, Scaling and intermittency in compressible isotropic turbulence, Phys. Rev. Fluids **2**, 053401 (2017).
[61] J. C. Vassilicos, Dissipation in turbulent flows, Annu. Rev. Fluid Mech. **47**, 95 (2015).
[62] G. L. Eyink and T. D. Drivas, Cascades and Dissipative Anomalies in Compressible Fluid Turbulence, Phys. Rev. X **8**, 011022 (2018).
[63] S. Pan and E. Johnsen, The role of bulk viscosity on the decay of compressible, homogeneous, isotropic turbulence, J. Fluid Mech. **833**, 717 (2017).
[64] S. Lee, S. K. Lele, and P. Moin, Simulation of spatially evolving turbulence and the applicability of Taylor hypothesis in compressible flow, Phys. Fluids **4**, 1521 (1992).
[65] S. Lee, S. K. Lele, and P. Moin, Eddy shocklets in decaying compressible turbulence, Phys. Fluids **3**, 657 (1991).
[66] G. P. Zank and W. H. Matthaeus, The equations of nearly incompressible fluids. i. hydrodynamics, turbulence, and waves, Phys. Fluids **3**, 69 (1991).

[67] V. Yakhot and Diego A. Donzis, Emergence of Multiscaling in a Random-Force Stirred Fluid, Phys. Rev. Lett. **119**, 044501 (2017).
[68] V. Yakhot and D. A. Donzis, Anomalous exponents in strong turbulence, Physica D **384-385**, 12 (2018).
[69] I. Staroselsky, V. Yakhot, S. Kida, and S. A. Orszag, Long-Time, Large-Scale Properties of a Randomly Stirred Compressible Fluid, Phys. Rev. Lett. **65**, 171 (1990).
[70] R. H. Kraichnan, On the statistical mechanics of an adiabatically compressible fluid, J. Acoust. Soc. Am. **27**, 438 (1955).